This article has been accepted for publication in a future issue of this journal, but has not been fully edited. Content may change prior to final publication.
Citation information: DOI: 10.17775/CSEEJPES.2021.03200, CSEE Journal of Power and Energy Systems

Intelligent Breakage Assessment of Composite Insulator on Overhead Transmission Line by Ellipse Detection Based on IRHT

Zhikang Yuan, *Member*, *IEEE&CSEE*, Linxuan He, Shaohe Wang, Youping Tu, Zhaojing Li, Cong Wang and Fan Li

***Abstract*—With the development of unmanned aerial vehicle (UAV) technology, visible image is playing an important role in maintenance of the power system. To achieve the shed breakage evaluation of composite insulator by UAV visible image, an intelligent fault assessment method is proposed. Firstly, the composite insulators in visible light images are identified by Faster-RCNN. After image preprocessing, the image is enhanced and the noise is removed. Then, the canny operator is used to extract the edge of the sheds. Improved Randomized Hough Transform (IRHT) is used to detect the ellipses in the edge image. The parameters of the detected ellipse, length of major axes and minor axes, center coordinates and deflection angle of major axes, are used to realize the segmentation of composite insulator. Finally, the number of pixel points in the ellipse and the distance between the points and the ellipse boundary are used to judge whether there are breakage or cracks on sheds. The area ratio of the breakage to the whole shed is calculated based on the number of pixel points inside the broken area. The method can be realized without large amount of training dataset of the specific fault type and provides a technical basis for the online fault assessment of composite insulator on overhead transmission line.**

***Index Terms*—composite insulator, breakage assessment, Improved Randomized Hough Transform (IRHT), ellipse detection.**

I. Introduction

COMPOSITE insulator, as an important component on overhead transmission line, is widely used due to its light weight and good hydrophobicity [1], [2]. With the development of UAV technology, visible image captured by UAV is playing an important role in power system operation and maintenance [3], [4], [5]. At present, although there are a lot of work on equipment detection and identification, the technology of fault diagnosis is still not mature based on the visible images.

Breakage of the sheds and housings, a typical fault of composite insulator, will not only shorten the flashover distance but also lead to abnormal temperature rise [6], [7]. There are many methods to detect the breakage, even the defects inside the composite insulators, such as infrared imaging [8], [9], ultrasound [10], [11]. The method based on visible images has high development potential because the images are easy to be obtained. Some scholars have made efforts in this aspect. Liu et al. [12] proposed a method to detect the cracks of composite insulators based on edge detection. Liu et al. [13] achieved the detection of cracks on composite insulators through ART-2 neural network and equidistant features. Quan [14] realized the detection of cracks on sheds of composite insulator through SVDD classifier. Huang et al. [15] realized the breakage detection of sheds on insulator by curve fitting. These works contribute greatly on breakage detection of composite insulator. However, the methods above are all based on machine learning, which requires large amount of training dataset of the specific fault type. As is known, composite insulators with fault are rare and it’s a hard work to obtain enough dataset cases. On the other hand, these methods can only be used to detect whether there is breakage of the sheds, but cannot be used to assess the fault quantitatively.

Image segmentation is a method to extract the insulator from the background. Combining with edge detection, image segmentation can be used to detect the breakage and cracks on the sheds. It shows promising potential to realize the evaluation of the breakage based on visible image. Image segmentation can be realized by color characteristics [16], gray thresholds [17], edge detection [19] and wavelet transform [20]. Jin et al. [16] achieved the segmentation of composite insulators by extracting the chromaticity and saturation of the visible image. Jiang et al. [17] turned the visible image to gray-scale image and segment the composite insulator according to gray threshold. Yu et al. [18] achieved the segmentation of composite insulators by extracting the gray scale, shape and texture features of the insulators. Zhong et al. [19] realized the segmentation of insulator through histogram of edge direction and deformation model. In these methods, the segmentation will be affected greatly by the background. The more complex the background is, the worse the segmentation result will be. To evaluate the breakage of composite insulator by visible image,

Manuscript received April 24, 2021. (Corresponding author: Linxuan He)
Zhikang Yuan is with the School of Electronic and Information Engineering, Tongji University, Shanghai 201804, China (e-mail: zhikangyuan@tongji.edu.cn)
Linxuan He, Youping Tu, Zhaojing Li, Cong Wang are with the State Key Laboratory of Alternate Electrical Power System with Renewable Energy Sources, North China Electric Power University, Beijing 102206, China (e-mail: 18511696639@163.com; typ@ncepu.edu.cn; 18810919790@163.com; cong@ncepu.edu.cn).
Shaohe Wang is with State Grid Zhejiang Electric Power Research Institute, Hangzhou 310014, China (e-mail: volk-hyllow@hotmail.com).
Fan Li is with State Grid Jiangxi Electric Power Research Institute, Nanchang 330000, China (e-mail: 798090132@qq.com).

This article has been accepted for publication in a future issue of this journal, but has not been fully edited. Content may change prior to final publication.
Citation information: DOI: 10.17775/CSEEJPES.2021.03200, CSEE Journal of Power and Energy Systems

it is important to find a new method that can extract the insulator from the background precisely.

In this paper, a method based on Improved Randomized Hough Transform (IRHT) is proposed to assess the breakage of shed on composite insulator in UAV visible image. This method can realize the detection of cracks, half breakage and breakage of sheds on composite insulators through image preprocessing, edge detection, ellipse detection, segmentation and breakage evaluation and also achieve the quantitative characterization of breakage.

The contributions of the work can be condensed as follows: 1. It achieves a high recognition rate of different breakage types of composite insulators with few breakage samples comparing with the popular methods, deep learning and machine learning, which need a large number of breakage samples with different types and degrees for training. 2. It realizes quantitative calculation on the breakage area of the sheds for the first time, which would supply the basis for insulator maintenance strategy according to the existing standard, DL/T 257-2012 [21]. On the other hand, the breakage area is related to the creepage distance of the insulator directly and the method can be used to evaluate the flashover risk of the insulator.

II. Method

A. Image preprocessing

Composite insulators are exposed to the open air and there are always trees, farmlands, etc. in the visible images as the background. On the other hand, light and electromagnetic interferences will also influence the image quality. Therefore, image preprocessing is carried out for the collected images to reduce the interferences and improve the image contrast, laying a foundation for fast and accurate identification of the sheds breakage. Image preprocessing is generally divided into four steps, which are object detection, graying, image denoising and image enhancement.

Deep learning is a common method to recognize the composite insulators in the images. According to the analysis of different deep learning models, YOLO is a single-stage target detection method, which is more suitable for real-time monitoring. However, the shape, size and other characteristics of the insulators are different in the captured images, leading to a low detection accuracy. Faster-RCNN is a two-stage target detection method with high detection accuracy. On the basis of Fast-RCNN, RPN, which is used to generate candidate regions, can greatly improve the detection speed. In this paper, Faster R-CNN and VGG-16 network [22] is used to recognize composite insulators in the visible images. The process is divided into five processes: image input, extraction of image features by VGG-16 network, generation of accurate candidate areas by RPN, fault type classification and regression calculation to obtain the detection frame of composite insulator. 800 images of composite insulators captured by UAV are selected as the training set of Faster-RCNN network. The test results show that this method can accurately identify the composite insulators in the images. Then the region, containing the composite insulator, in the image is segmented as the follow-up research object.

The weighted average method is adopted to realize the graying of the original image. The specific expression is shown in (1),

$$gray = R\times 0.299 + G\times 0.587 + B\times 0.114 \tag{1}$$

where $gray$ is the gray value of the pixel, and R, G, and B are the red, green, and blue values of the original image, which are from 0 to 255.

Gaussian filter is used to remove the noise. The main idea is to use a Gaussian template to convolve with the image. The value of the center point is determined by the weighted average. The convolution is shown in (2),

$$I_\sigma = I * G_\sigma \tag{2}$$

where I_σ is the image after filtering, and G_σ is a gaussian template with a standard deviation of σ. Gauss template is defined as (3),

$$G_\sigma = \frac{1}{2\pi\sigma} e^{-(\frac{x^2+y^2}{2\sigma^2})} \tag{3}$$

where x^2 and y^2 represent the distance between the pixels in the center neighborhood of the gaussian template and the pixels in the center of the template, respectively.

Histogram equalization of grayscale images is the most used image enhancement method. For a discrete image, the probability of the i-th gray level r_i can be calculated by following (4),

$$P_r(r_i) = \frac{m_i}{m} \tag{4}$$

where m_i is the number of pixels appearing at level r_i. m is the total number of pixels. The histogram equalization of the image is shown in (5),

$$S_i = T(r_i) = \sum_{i=0}^{k=1} P_r(r_r) = \sum_{i=0}^{k=1} \frac{m_i}{m} \tag{5}$$

where S_i is the number of pixel points in the i-th gray level and k is the gray level series.

B. Edge detection

The edge information of the image is particularly important, which can be used to extract the sheds of the composite insulators.

Canny operator [23] has been widely used in various fields due to its advantages of low misjudgment rate, high precision and suppression of false edge. In this paper, canny operator is used to extract the edge of composite insulators. However, due to the existence of pollution or pulverization, the results of edge detection show not only the edge of sheds, but also the edge of pollution and pulverization. However, the gray value of the edges is lower than that of the sheds. We use binarization to remove the influence of pollution and pulverization on edge detection. In the binarization method, threshold is a critical factor that influence the result, which can be obtained by OTSU [24], [25]. In order to select an appropriate threshold, this paper compares the results of fixed threshold with those obtained by OTSU, which will be analyzed in chapter 3.

This article has been accepted for publication in a future issue of this journal, but has not been fully edited. Content may change prior to final publication.
Citation information: DOI: 10.17775/CSEEJPES.2021.03200, CSEE Journal of Power and Energy Systems

The steps of edge detection are as follows.

1) Calculate the magnitude and direction of the gradient of the filtered image. The expressions are shown in (6), (7), respectively.

$$M(i,j)=\sqrt{k_x^2(i,j)+k_y^2(i,j)} \tag{6}$$

$$H(i,j)=\arctan[k_x(i,j),k_y(i,j)] \tag{7}$$

2) Apply non-maximum suppression to the gradient amplitude.
3) Use double threshold algorithm to detect and connect edges, in which the high threshold is 0.8 and the low threshold is 0.2.
4) Binarize the edge image.
5) Thin the edge.

C. Ellipse detection

Due to the shooting angle, the shape of the composite insulator shed in the image captured by UAC is always oval. Randomized Hough transform is a common method to find the targets with fixed geometries, which is widely used on detection of lines, circles and ellipses in image. In this paper, Improved Randomized Hough transform (IRHT) [26] was put forward to detect the sheds. The main idea is that 3 edge points in the edge image are randomly selected and fitted as an ellipse. Then, a 4th edge point is used to verified the correctness of the fitted ellipse. The specific steps of IRHT are as follows and are shown in Fig. 1.

1) Add all edge points into set V at first. z is defined as the initial number of edge points in set V. n_p is the number of the edge points that left in set V. Set three counters, f=0, a=0, T_0=0. Then, five thresholds, T_f, T_a, T_d, T_{em}, and T_r are defined. T_f is the maximum number of failures that can be tolerated. T_a is shortest distance between two of the randomly selected three edge points that can be allowed. T_d is longest distance from the 4th point in the boundary of the ellipse that can be allowed. T_{em} is the minimum value of n_p/z. T_r is minimum ratio of the detected pixel number on the boundary of the ellipse and the pixel number on the boundary of the ideal ellipse. T_d can be obtained by following (8),

$$\begin{cases} T_d=|ax_A^2+bx_Ay_A+cy_A^2+dx_A+ey_A+1| \\ x_A=x_0+(A+d_{diff})\cos\varphi \\ y_A=y_0+(A+d_{diff})\sin\varphi \end{cases} \tag{8}$$

where (u_0, v_0) is the coordinate of the center point of the ellipse, d_{diff} is the maximum distance from the edge point to the ellipse boundary, A and φ are the length of the major axes and the deflection angle of the major axes, respectively.

2) When $f<T_f$ and $n_p \geq zT_{em}$, 4 random points are selected and removed from V. Otherwise, the algorithm will be terminated.
3) According to 3 of the selected edge points, a possible ellipse can be obtained. The shortest distance between two of the 3 edge points (D_1) should be larger than T_a. The shortest distance between the 4th point to the boundary of the ellipse (D_2) should be less than T_d, as well. Otherwise, the selected 4 edge points will be moved back to set V and f=f+1.
4) Find out the edge points, the distances between whom to the boundary of the ellipse are less than T_d in set V. Use a to count the point number. n_{old} is the collected point number.
5) If $n_{old}>T_r\cdot C_{ijk}$, where C_{ijk} is the pixel number of the boundary of the ellipse, build a new set V_e. to collect the edge points, whose distances to the boundary of the ellipse are less than d_{diff}, in set V. Otherwise, move the 4 points back to set V and f=f+1.
6) Use the edge points in set V_e to fit a new ellipse as step 3) shows. The number of the edge point on the boundary of the new ellipse is n_{new}. Then, T_0=T_0+1.

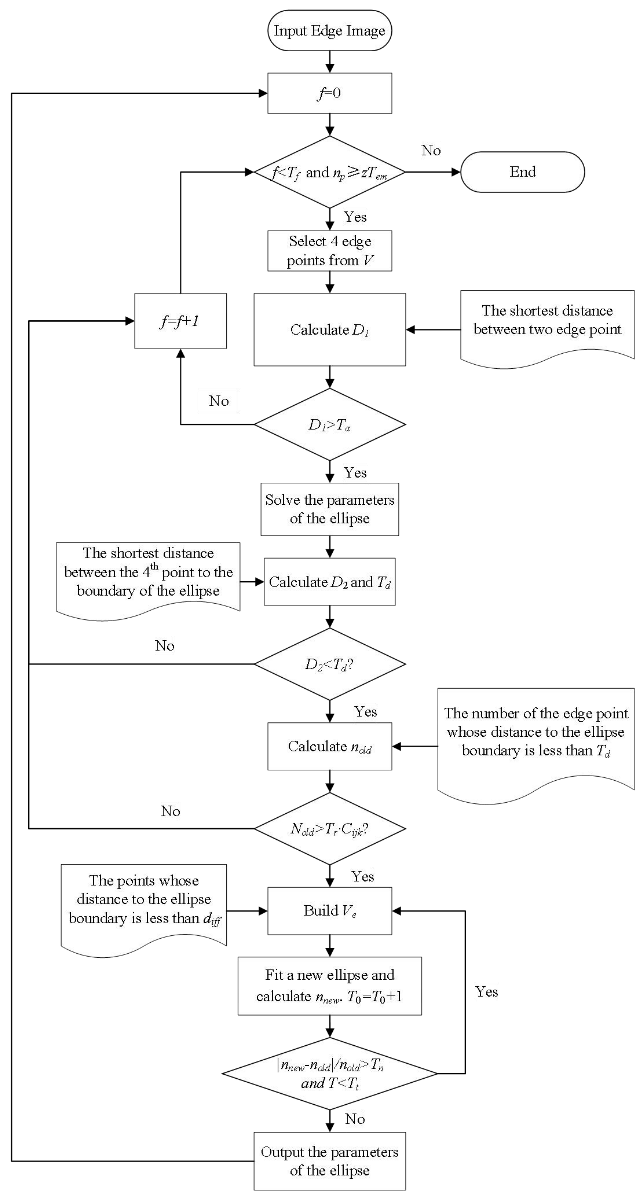

Fig. 1. Flow chart of ellipse detection based on IRHT.

7) Define the maximum number of iterations and the minimum rate of change as T_t and T_n, respectively. T_t=5 and T_n=0.1 in this work. If $|n_{new}-n_{old}|/n_{old}>T_n$ and $T_0<T_t$, then jump to step 6). Otherwise, V=V-V_e, f=0, and output the parameters of the ellipse.

This article has been accepted for publication in a future issue of this journal, but has not been fully edited. Content may change prior to final publication.
Citation information: DOI: 10.17775/CSEEJPES.2021.03200, CSEE Journal of Power and Energy Systems

8) Go back to step 2) to find the other ellipses in the image.

D. Segmentation

The parameters of ellipse, including the lengths of major axes and minor axes, center coordinate and deflection angle of major axes, can be obtained by IRHT. Then, we set the pixels outside the ellipse to white to realize the segmentation of the shed. The specific steps are as follows.

1) Transform the image obtained by object detection from the Red, Green, Blue (RGB) color model to the Hue, Saturation, Value (HSV) model.
2) Traverse the entire image and set H, S and V component of pixels which are not in any ellipse as 0°, 0 and 1.

The segmentation method proposed in this paper is based on the shape characteristics of the composite insulators. Once the ellipses are found, the composite insulator can be easily divided from the background. The traditional method based on color threshold cannot segment the composite insulator precisely. There are always background information especially at the edge of the composite insulator.

E. Breakage evaluation

There are three typical forms of breakage on the sheds of composite insulator, which are crack, half-breakage and breakage, as shown in Fig. 2.

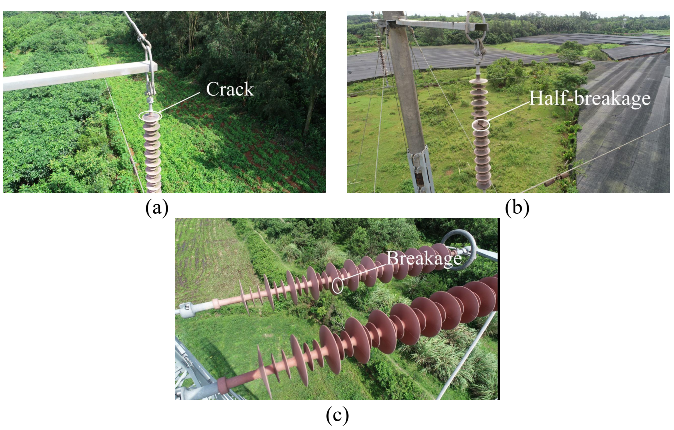

Fig. 2. Three typical forms of breakage. (a) cracks, (b) half-breakage, and (c) breakage.

The crack of the shed is shown in Fig. 2(a). The shed keeps the original shape even though there is crack on the surface. Half-breakage means that part of the shed is broken but still connects to the composite insulator, as shown in Fig. 2(b). Breakage is a condition that the broken area of the shed has fallen off as shown in Fig. 2(c).

When the sheds of composite insulator are broken, there will be detected edge in the ellipse. Breakage detection can be realized by analyzing the distance between the edge point of the broken area and the ellipse boundary. The specific steps are as follows.

1) Select a detected ellipse, traverse the whole image to search the edge points inside the ellipse.
2) Estimate whether these edge points are on the boundaries of the other ellipses and, if so, remove the edge points.
3) Calculate the distance D between the reserved edge points and the boundary of the selected ellipse. If $D>y_A\cdot 3\%$ (y_A is the length of minor axes), The counter $N=N+1$. If $N>100$, it is considered that there is breakage or crack in the shed.
4) Find the pixel point in the reserved edge points, which shows the smallest distance to the ellipse boundary, and calculate the distance D_{avg1}. If $D_{avg1}>y_A\cdot 5\%$, the breakage type is considered as crack.
5) Find the pixel point at the other end of the reserved edge line, and calculate the distance from the point to the nearest point of ellipse boundary D_{avg2}. If $D_{avg2}<y_A\cdot 5\%$, it is considered that there is breakage on the shed. Otherwise, the breakage type is defined as half-breakage.

The flow chart to assess the breakage type of the shed is presented in Fig. 3.

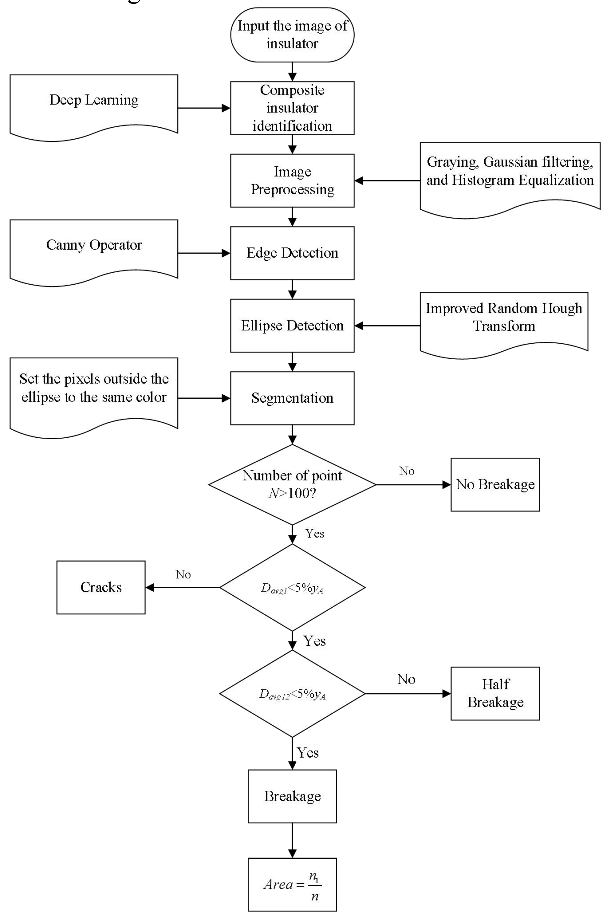

Fig. 3. Flow chart of breakage assessment of composite insulator shed.

Then, we are going to calculated the area ratio of the broken area. The main idea is to find out the percentage of pixel number in the broken, which follows (9),

$$S=\frac{n_1}{n} \tag{9}$$

where n_1 is the number of pixels in the broken area, and n is the number of pixels in the ellipse. The specific steps are as follows.

1) Select the shed, where breakage has been detected, and obtain the pixel number n in the ellipse.
2) Find the pixel point in the reserved edge points, which is the nearest to the center point of the ellipse, and establish a

This article has been accepted for publication in a future issue of this journal, but has not been fully edited. Content may change prior to final publication.
Citation information: DOI: 10.17775/CSEEJPES.2021.03200, CSEE Journal of Power and Energy Systems

direction vector to indicate the position relationship between the pixel point and the elliptic center.

3) Obtain the pixel number n_1 between the reserved edge points and the boundary of the selected ellipse in the direction of the direction vector.

III. Parameter Setting

A. Gaussian filter and binarization

In image processing, the Gaussian filtering results will be affected by the standard deviation σ of the Gaussian tamplate. The larger the standard deviation is, the greater the smoothing effect is. However, large standard deviation will lead to image distortion. Similarly, in the process of binarization, the lower the threshold T is, the more the edge information in the image is. However, the edges of pollution and pulverization will also be highlighted with the decrease of the threshold. Therefore, it is important to find the appropriate standard deviation and threshold in the Gaussian filter and bunarization stages.

To evaluate the image processing effect under the conditions with different standard deviations and thresholds, N_1 and N_2, which represent the shed recognition rate and error detection rate of the fault type of composite insulator influenced by the pollution and pulverization, respectively, are put forward. Images of 50 composite insulators are selected for testing. The values of N_1 and N_2 with different standard deviations and thresholds are shown in Tab. I and Tab. II, respectively.

TABLE I
Result of N_1 under Different Standard Deviations and Thresholds

	σ=0.6	σ=0.8	σ=1.0	σ=1.2
T=0.1	73.54%	75.81%	71.39%	68.16%
T=0.2	76.36%	81.24%	78.61%	78.34%
T=0.3	68.49%	71.22%	67.53%	65.74%
OTSU	74.57%	77.42%	76.47%	75.83%

TABLE II
Result of N_2 under Different Standard Deviations and Thresholds

	σ=0.6	σ=0.8	σ=1.0	σ=1.2
T=0.1	12%	8%	10%	10%
T=0.2	4%	0	2%	4%
T=0.3	0	0	2%	2%
OTSU	6%	2%	2%	4%

From Tab. I, it is found that N_1 doesn't show monotonic change with the standard deviation or threshold. When the threshold of binarization is fixed at 0.2, the shed recognition rate is higher than the other conditions. On this basis, when the standard deviation of Gaussian filter is 0.8, the shed recognition rate can even reach to 81.24%, which is the highest in Tab. I. In Tab. II, when the threshold of binarization is 0.3, there is no error detection of the fault type of composite insulator. As the threshold decrease from 0.3 to 0.1, the error detection rate rises from 0 to 12% when the standard deviation of Gaussian filter is 0.2. The reason is that a lower threshold of binarization enhances the influence effect of background, pollution and pulverization. When the threshold is determined by OTSU, the error detection rate is 6%. It can be concluded as the best strategy when the standard deviation of Gaussian filter is 0.8 and the threshold of binarization is 0.2. The shed recognition rate is 81.24% and there is error detection of the fault type.

B. Parameters for ellipse detection

In the process of parameter selection of ellipse detection, the suggested values of T_f and T_{em} are 5000 and 0.1, respectively, according to Ref. [25].

The pixel size of the shed major axes in the image is about 200, while the pixel size of minor axes is about 30. According to the ellipse detection requirements of the algorithm, T_a is set to 30.

Parameter T_r, the threshold of ellipse defect rate ranging from 0 to 1, is critical for the ellipse detection of the shed. When T_r is too small, the detected ellipse may be over segmented, dividing the real ellipse into several small pieces. On the other hand, when T_r is too large, it may lead to the detection failure of the small sheds which are partially covered by the other sheds. In this section, N_1, the shed recognition rate, is also employed to obtain the appropriate value of T_r. The result of N_1 under different thresholds of ellipse defect rate are shown in Tab. III.

TABLE III
Result of N_1 under Different Thresholds of Ellipse Defect Rate

T_r	0.3	0.4	0.5	0.6	0.7
N_1	71.35%	75.58%	81.82%	67.16%	60.65%

As T_r rises from 0.3 to 0.5, N_1 also increases from 71.35% to 81.82%. When T_r=0.5, the shed recognition rate reaches the maximum value. Then, the shed recognition rate decreases rapidly with the increase of T_r. When T_r=0.7, N_1 drops to 60.65%. Therefore, we set T_r to 0.5.

IV. Result and Analysis

The composite insulator recognition based on Faster-RCNN runs under the following computer configuration: Windows 10 operating system, Intel Xeon Gold 5120T CPU (2.20GHz×16), GeForce RTX 2080Ti graphics card, and TensorFlow. And the other algorithms run under the following computer configuration: Windows 10 operating system, Intel Core i5 9400 CPU (2.90GHz×6), and GeForce GTX 1060Ti graphics card.

A. Results

28 images of 35 kV composite insulators, and 29 images of 110 kV composite insulators are used to verify the effectiveness of the proposed method. Fig. 4 shows 8 composite insulators with different operation states. The detected results are also presented in each figure. The targets in Fig. 4(a), 4(b) and in the left of 4(g) are composite insulators with no breakage. Cracks on the sheds are found in the composite insulators and highlighted by white boxes in Fig. 4(c) and 4(d). The composite insulators show half breakage on sheds in Fig. 4(e) and 4(f). In Fig. 4(g) and 4(h), the breakage parts of the composite

This article has been accepted for publication in a future issue of this journal, but has not been fully edited. Content may change prior to final publication. Citation information: DOI: 10.17775/CSEEJPES.2021.03200, CSEE Journal of Power and Energy Systems

insulators are also highlighted in white boxes. What's more, the breakage areas have been calculated and marked near the white box.

Take Figure 4(d) as an example, the detection process is presented in Fig. 5. At first, target detection based on Faster-RCNN is conducted and the composite insulator is detected, as shown in Fig. 5(a). Secondly, we obtain Fig. 5(b), a gray image of the composite insulator, by image preprocessing. Then, Canny operator is used to detected the edge of the insulator. Considering that the pollution on the sheds may be detected as edges, binarization of the edge detection results is conducted to remove the erroneous edges. The image after binarization is shown in Fig. 5(c). Through ellipse detection, the shed contour of the composite insulator can be found. However, two small sheds, the second and sixth shed from the low voltage end, are missing in Fig. 5(d). This is because the shooting position of the UAV is too high to obtain each shed contour accurately, which informs that the shooting position and angle will influence the working efficiency directly. Next, the background can be removed by segmentation, as shown in Fig. 5(e). Following the step of breakage evaluation, the breakage type can be identified and the breakage area is highlighted in red box in Fig. 5(f). So as to the detection time, the target detection by deep learning costs 0.531s. The total time of the other steps are only 0.415s.

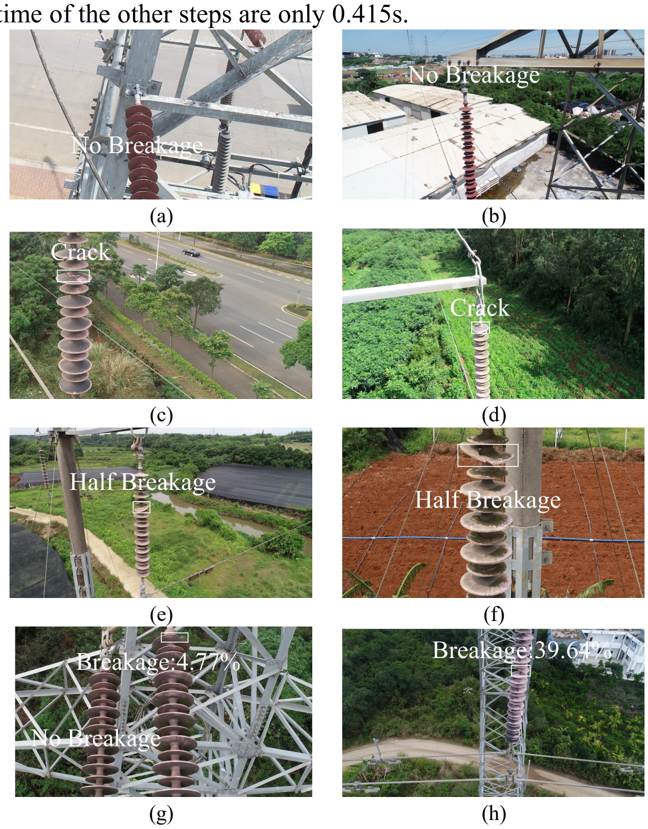

Fig. 4. Image of composite insulators. (a), (b) no breakage, (c), (d) crack, (e), (f) half-breakage, (g), (h) breakage.

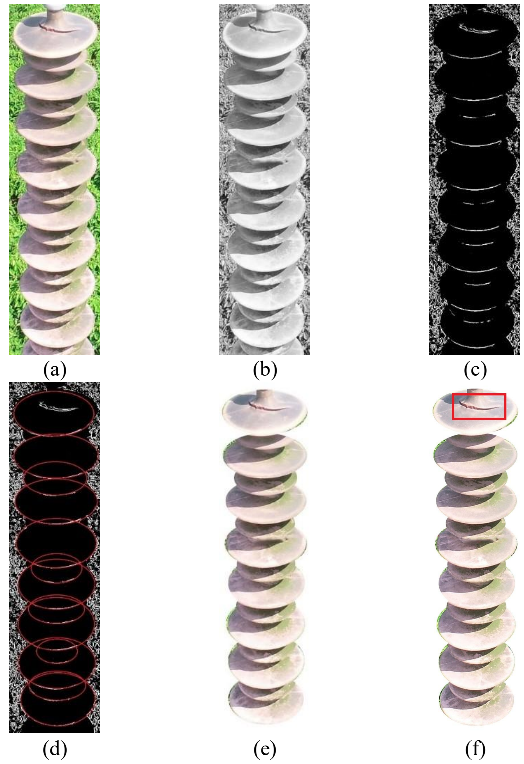

Fig. 5. Breakage detection process. (a) object detection, (b) image preprocessing, (c) edge detection, (d) ellipse detection, (e) segmentation, and (f) broken area marking.

TABLE IV
DETECTED RESULTS OF COMPOSITE INSULATOR

Voltage	Operation state	Detected results			
		No breakage	Crack	Half breakage	Breakage
35 kV	No breakage	16	2	0	1
	Crack	0	3	0	0
	Half breakage	0	0	2	0
	Breakage	0	0	0	4
110 kV	No breakage	8	3	0	2
	Crack	0	6	0	0
	Half breakage	0	0	3	0
	Breakage	0	0	0	7

The detected results of all the composite insulators in the images are shown in Tab. IV. It is found that crack and breakage of the shed can be identified and quantitatively assessed. However, some sheds with no breakage have been detected as crack or breakage sheds. Crack and breakage are found in three 35 kV composite insulators and five 110 kV composite insulators with no breakage. There are several reasons for the error detection. Firstly, the shadow will be detected as breakage on the shed when the image is taken in sunlight. It cannot be removed in binarization stage and there is still no effective image enhancement method to get rid of the shadow. It is suggested to avoid taking visible images of composite insulator in sunlight for breakage assessment. On the other hand, the pollution with clear edge on shed may be detected as breakage. For the composite insulator with breakage, no matter what type of the breakage is, the method proposed in this paper can be used to achieve the detection. This is because when there is breakage on sheds of composite insulator, the edge of the breakage area will only appear inside

This article has been accepted for publication in a future issue of this journal, but has not been fully edited. Content may change prior to final publication.
Citation information: DOI: 10.17775/CSEEJPES.2021.03200, CSEE Journal of Power and Energy Systems

the ellipse.

The correct recognition rate of composite insulators with different fault types by the proposed method are summarized in Tab. V. It also shows the correct recognition rates of the other methods, including ART-2 neural network with equidistant feature in Ref. [13] and SVDD classifier in Ref. [14]. Both the methods in the references are based on machine learning, which needs a large database of crack and breakage samples for training. Though the case numbers of crack, half breakage and breakage in this paper are only 9, 5 and 11, respectively, 100% correct recognition rate has been achieved by the proposed method in this paper. What's more, the proposed method can even realize the quantitative assessment of the breakage area, which cannot be achieved by the methods of machine learning.

TABLE V
RECOGNITION RATE OF DIFFERENT METHOD

Method	No breakage	Crack	Half breakage	Breakage
ART-2 by Liu [13]	95.0%	85.0%	-	-
SVDD by Quan [14]	-	90.0%	-	86.7%
Method in this paper	75.0%	100%	100%	100%

It's worth noting that the pixel sizes of these images are about 5472×3078. Due to the different image shooting conditions of UAV, the pixel size of composite insulator in the image varies a lot. If the pixel size is not large enough, the edge of composite insulator will be blurred, which will influence the results of edge detection and ellipse detection directly. Till now, the minimum pixel size of the insulator for detection requirements is still unclear. On the other hand, the shooting position and angle of UAV also matter in the process of edge detection. There is still no standard or mature rule for UAV imaging. We are going to pay attention on these two aspects in the following work.

In DL/T 257-2012 [21], it is mentioned that composite insulator will be replaced when the number of shed, which contains breakage, exceeds 1/3. The method proposed in this paper cannot only help to evaluate the operation state of composite insulator based on existing standard, but also holds the possibility to realize further classification of the operation state of composite insulator for its ability of quantitative assessment.

B. Model sensitivity test

Due to the small size of sample dataset used in this paper, overfitting may occur in this model. We carry out the model sensitivity test by data augmentation. Different methods of data augmentation, including rotation, mirror flipping, and brightness change of the image, are used for the sample at random. The method of data augmentation and parameters are shown in Tab. VI. A total 146 images were obtained by data augmentation.

TABLE VI
METHODS FOR DATA AUGMENTATION

Method	Parameter
Rotation	Clockwise 30 °, Anticlockwise 30 °
Mirror Flipping	Horizontal, Vertical
Changing the Brightness	Brightness of the original:120%, 150%

TABLE VII
DETECTED RESULTS OF COMPOSITE INSULATOR

Voltage	Operation state	Detected results			
		No breakage	Crack	Half breakage	Breakage
35 kV	No breakage	42	5	0	2
	Crack	0	10	0	0
	Half breakage	0	0	5	0
	Breakage	0	0	0	9
110 kV	No breakage	23	7	0	5
	Crack	0	15	0	0
	Half breakage	0	0	6	0
	Breakage	0	0	0	17

The detected results of all the composite insulators after data augmentation are shown in Table VII and summarized in Table VIII. Some sheds with no breakage are still detected as crack or breakage sheds. The recognition rate is 77.4%, which is close to the recognition rate before data augmentation, 75.0%. The recognition rates of the composite insulators with crack, half breakage and breakage are all 100%. Data augmentation doesn't influence the recognition rate of the composite insulators with crack or breakage. The results show that the method proposed in this paper has no over-fitting problem even though the sample size of the data is small.

TABLE VIII
RECOGNITION RATE AFTER DATA AUGMENTATION

	No breakage	Crack	Half breakage	Breakage
Recognition Rate	77.4%	100%	100%	100%

V. CONCLUSION

In this study, an intelligent fault assessment method for composite insulator based on visible image captured by UAV is proposed. Four steps, image preprocessing, edge detection, ellipse detection and segmentation, are included before fault diagnosis. The values of standard deviation of the Gaussian template and the binarization threshold have been discussed, which are suggested to be fixed at 0.8 and 0.2, respectively. This method can distinguish three typical faults of sheds, crack, half breakage and breakage, without large amount of training dataset of the specific fault type. Furthermore, it can realize the quantitative evaluation of the breakage area, which provides a new idea for online fault assessment of composite insulator on overhead transmission line. In future work, we will study the influence of image clarity on breakage detection of composite insulator. And the effect of the UAV shooting conditions on the detection results will also be studied.

REFERENCES

[1] R. Hackam, "Outdoor HV composite polymeric insulators," *IEEE Trans. Dielectrics and Electrical Insulation*, vol. 6, pp. 557-585, 1999.
[2] S. Li, S. Yu and Y. Feng, "Progress in and prospects for electrical insulating materials," *High Voltage*, vol. 1, no. 3, pp. 122-129, 2016.
[3] L. Liu, C. Guo, Y. Tu, H. Mei and L. Wang, "Differential Evolution Fitting-Based Optical Step-Phase Thermography for Micrometer

This article has been accepted for publication in a future issue of this journal, but has not been fully edited. Content may change prior to final publication. Citation information: DOI: 10.17775/CSEEJPES.2021.03200, CSEE Journal of Power and Energy Systems

Thickness Measurement of Atmospheric Corrosion Layer," *IEEE Trans. Industrial Informatics,* vol. 16, no. 8, pp. 5213-5222, 2020.
[4] L. Xin, H. Jin, Y. Tu, Z. Yuan, Z. Lv and C. Wang, "Defect Detection and Characterization of RTV Silicone Rubber Coating on Insulator Based on Visible Spectrum Image," *IEEE Trans. Power Delivery*, DOI: 10.1109/TPWRD.2020.2995071.
[5] H. Mei, X. Guan, X. Fu, C. Zhao and L. Wang, "Influence of tower anticorrosion coating as contaminant on operation characteristics of composite insulator," *High Voltage*, vol. 3, no. 3, pp. 193-198, 2018.
[6] Z. Yuan, Y. Tu, Y. Zhao, H. Jiang and C. Wang, "Analysis on Heat Source of Abnormal Temperature Rise of Composite Insulator Housings," *IEEE Trans. Dielectrics and Electrical Insulation*, vol. 24, no. 6, pp. 3578-3585, 2017.
[7] Z. Yuan, Y. Tu, R. Li, F. Zhang, B. Gong and C. Wang, "Review on characteristics, heating sources and evolutionary processes of the operating composite insulators with abnormal temperature rise," *CSEE Journal Power and Energy Systems*, DOI: 10.17775/CSEEJPES.2019.02790.
[8] M. Akyuz, L. Gao, V. Cooray, T. G. Gustavsson, S. M. Gubanski and A. Larsson, "Positive streamer discharges along insulating surfaces," *IEEE Trans. Dielectrics and Electrical Insulation*, vol. 8, no. 6, pp. 902-910, 2001.
[9] M. Vitelli, V. Tucci and C. Petrarca, "Temperature distribution along an outdoor insulator subjected to different pollution levels," *IEEE Trans. Dielectrics and Electrical Insulation*, vol. 7, no. 3, pp. 416-423, 2000.
[10] H. Wang, L. Cheng, R. Liao, S. Zhang and L. Yang, "Non-destructive testing method of micro-debonding defects in composite insulation based on high power ultrasonic," *High Voltage*, vol. 4, no. 3, pp. 167-172, 2019.
[11] H. Wang, L. Cheng, R. Liao, S. Zhang and L. Yang, "Nonlinear ultrasonic nondestructive detection and modelling of kissing defects in high voltage composite insulators," *IEEE Trans. Dielectrics and Electrical Insulation*, vol. 27, no. 3, pp. 924-931, 2020.
[12] H. Liu, X. He, X. Liu. "Research on Computer Application of Image Segmentation Algorithm based on Watershed and Region Merging," *Computer application research*, vol. 24, no. 9, pp. 307-308, 2007.
[13] G. Liu, Z. Jiang. "Recognition of porcelain bottle crack based on modified ART-2 network and Invariant moment," *Scientific Instruments*, vol. 30, no. 7, pp. 1420-1425, 2009.
[14] W. Quan, "Research on key technology of insulator surface breakage detection based on image processing," M.S. thesis, Dept. Elect. Chi., HIT Univ., Harbin, China, 2019.
[15] X. Huang, F. Zhang. "Suspension Insulator String Damage Detection Technology Based on Curve Fitting," *High Voltage Apparatus*, vol. 51, no. 11, pp. 116-121, 2015.
[16] S. Ma, J. An, F. Chen. "Segmentation of the Blue Insulator Images Based on Region Location," *Electric power construction*, vol. 31, no. 7, pp. 14-17. 2010.
[17] H. Jiang, L. Jin, S. Yan. "Recognition and fault diagnosis of insulator string in aerial images," *Mechanical and electrical engineering*, vol. 32, no. 2, pp. 274-278. 2015.
[18] L. Yu, B. Yao, W. Wu. "Insulator Identification Method Based on Multi-feature," *Insulators and Surge Arresters*, no.3, pp. 79-83. 2016.
[19] L. Zhong, H. Feng, L. Sui. "An Insulator Detection Method Using Edge Orientation Histogram," *Electrical technology*, no.1, pp. 22-25. 2010.
[20] T. Wan, N. Canagarajah and A. Achim, "Segmentation of noisy color images using Cauchy distribution in the complex wavelet domain," *IET Image Processing*, vol. 5, no. 2, pp. 159-170, 2011.
[21] Installation, operation and maintenance specification of composite insulators for a.c. and d.c. overhead lines with a nominal voltage greater than 1000 V, DL/T 257-2012, 2012
[22] W. Wu, Y. Yin, X. Wang and D. Xu, "Face Detection with Different Scales Based on Faster R-CNN," *IEEE Trans. Cybernetics*, vol. 49, no. 11, pp. 4017-4028, 2019.
[23] W. Wang, G. Liu. Image edge detection of insulators. *Control & Automation*, vol. 24, no. 27, pp. 308-309, 2008.
[24] M. Dhimish and P. Mather, "Ultrafast High-Resolution Solar Cell Cracks Detection Process," *IEEE Trans. Industrial Informatics*, vol. 16, no. 7, pp. 4769-4777, 2020,
[25] N. Otsu, "A Threshold Selection Method from Gray-Level Histograms," *IEEE Trans. Systems*, Man, and Cybernetics, vol. 9, no. 1, pp. 62-66, 1979.
[26] L Li, Z Feng, K He. "An improved randomized algorithm for detecting ellipses based on least square approach," *Journal of Zhejiang University*. vol. 42, no. 8, pp. 1360-1364, 2008.

Zhikang Yuan (SM'17-M'19) was born in Quzhou, Zhejiang Province, China, in 1992. He received the BSc. and Ph.D. degree in electrical engineering from North China Electric Power University, Beijing, in 2014 and 2019, respectively. Currently, he is an assistant professor in the School of Electronic and Information Engineering at Tongji University in Shanghai, China. His research interests include outdoor insulation and smart dielectrics.

Linxuan He was born in Xingtai, Hebei Province, China, in 1997. He received the BSc. degree in control technology and instruments from North China Electric Power University, Beijing, in 2019. His research interests include outdoor insulation.

Youping Tu was born in Ningbo, Zhejiang, China, in 1966. She received her B.Sc. and M.Sc. degrees from the Department of Electrical Engineering, Chongqing University in Chongqing, China, respectively in 1988, and in 1991. Currently, she is a professor in the Department of Electrical Engineering at North China Electric Power University in Beijing, China. From 1991 to 1994, she worked in the computer application field in Hangzhou Heat Power Plant, Zhejiang Province, China. During 1994, she was a research assistant in the Department of Precision Instrument and Mechanics, Tsinghua University in Beijing, China. From 1994 to 1995, she worked in Ludao Company in Beijing, China. She was a lecturer from 1995 to 2003, and an associate professor from 2004 to 2010 in the Department of Electrical Engineering at North China Electric Power University in Beijing, China. Her research interest includes insulation technology, overvoltage and protection for power system. She is the author of more than 100 technical papers.

Zhaojing Li was born in Xiangyang, Hubei Province, China, in 1997. He received the BSc. degree in electric engineering from North China Electric Power University, Beijing, in 2019. His research interests include outdoor insulation.

Cong Wang was born in Ganzhou, Jiangxi Province, China, in 1980. He obtained his B.Sc., M.Sc., and Ph.D. degrees from the Department of Electrical Engineering, North China Electric Power University in 2002, 2012, and 2020, respectively, in Beijing, China. Currently, he is a senior engineer in the Department of Electrical Engineering, North China Electric Power University in Beijing, China. His research interests include properties of the dielectric material, gas discharge and online monitoring of electrical equipment.